A DATA-DRIVEN RANDOM WALK APPROACH FOR SOLVING WATER FLOW DYNAMICS IN SOIL SYSTEMS

Zeyuan Song [a,] and Zheyu Jiang [a 1]

[a] School of Chemical Engineering, Oklahoma State University, Stillwater, OK 74078

Abstract

Modeling and predicting soil moisture is essential for precision agriculture, smart irrigation, and drought prevention. In this work, we introduce a novel data-driven random walk (DRW) approach to solve n-dimensional Richards equation, a complex partial differential equation that characterizes water flow dynamics in soil. This advanced computational framework integrates multiple features, including finite volume discretization, adaptive L-scheme, multi-layer neural networks, and the concept of random walk to enable fast and accurate numerical solution of the Richards equation. Through an illustrative example, we demonstrate the accuracy and attractiveness of this novel approach. In particular, we show that our DRW approach can implicitly capture the underlying physical relationships among soil moisture content, pressure head, and flux, which will enable more accurate characterization of water flow dynamics.

Keywords

Soil moisture, partial differential equation, random walk, neural network, finite volume method.

Introduction

Soil moisture is a key hydrological state variable that has significant importance for the global environment and human society. In particular, accurate modeling and monitoring of root zone soil moisture in crop fields, which defines the amount of water stored within the plant root zone (top 100 cm of soil) available for transpiration and photosynthesis, is essential for improving agricultural production and crop productivity, providing basis for precision irrigation, preventing leaching of pesticides and soil nutrients into groundwater, and predicting agricultural droughts (Babaeian et al., 2019). Recent studies reveal that monitoring root zone soil moisture at suitable locations and adjusting irrigation schedules accordingly can reduce water use by 40-60% (Spelman et al., 2013) and increase farmer's revenue by 20-60% (Saavoss et al., 2016). Soil moisture level is also directly related to the concentration of fertilizers and pesticides in soil, which has profound environmental and food safety implications.

Estimating root zone soil moisture from surface or near-surface soil moisture data is typically achieved by solving a hydrological model that describes water movement through soils. Most of the advanced agro-hydrological models today incorporate the Richards equation (Richards, 1931), which captures irrigation, precipitation, evapotranspiration, runoff, and drainage dynamics of water in saturated and unsaturated

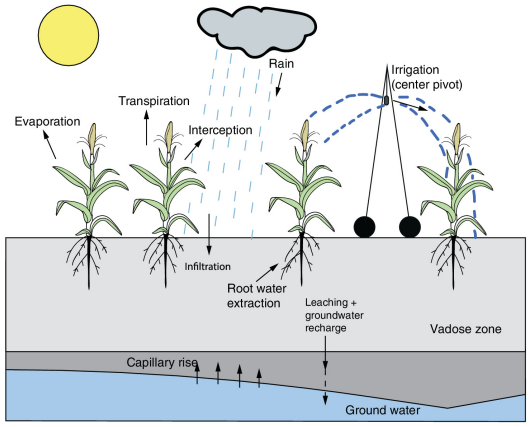

Figure 1: A schematic of agro-hydrological system (Source: Orouskhani et al. (2022)).

porous medium such as soil (Figure 1):

$$\partial_t \Theta(\psi) + \nabla \cdot \mathbf{q} = 0, \tag{1}$$

$$\mathbf{q} = -\mathbf{K}(\Theta)\nabla(\psi + z), \tag{2}$$

where ψ stands for pressure head, $\mathbf{q}$ is the flux, Θ denotes the moisture content, $\mathbf{K}$ is unsaturated hydraulic water conductivity, $t \in [0, T]$ denotes the time, and z denotes the vertical depth. In this work, we ignore the sink term associated with the root water extraction rate without loss of generality. For unsaturated flow, both Θ and $\mathbf{K}$ are functions of pressure head ψ and soil properties (Mualem, 1976; van Genuchten, 1980). In particular, small changes in Θ can change K by several orders of magnitude (Cockett et al., 2018). Thus, $\mathbf{K}(\Theta)$ is a highly nonlinear function, which makes Equation (1) very

[1] Corresponding author: Z. Jiang (E-mail: zheyu.jiang@okstate.edu).

difficult to solve in practice. Most existing Richards equation solvers use discretization approaches such as finite difference (Agyeman et al., 2021), finite element (Simunek et al., 2008), or finite volume (Healy, 2008). Unlike finite difference and finite element methods which no longer preserve useful physical information after discretization, the finite volume method (FVM) adopts an integral form of the Richards equation, which offers some valuable physical insights about water flow dynamics (Rathfelder and Abriola, 1994). However, even if the Richards equation is discretized using FVM, the discretized equations are transformed into a matrix equation and solved numerically, which lose the physical insights during solution process. Therefore, our goal is to enhance the quality and performance of the solution process by developing a novel computational framework that explores and utilizes the underlying physics behind the Richards equation.

To explore and incorporate additional useful physical insights to our algorithm, we introduce the concept of random walk, a stochastic process that describes the paths as N particles/molecules move in random steps, to the FVM framework to model water flow dynamics subject to external forces (*e.g.,* gravity) and obstacles. Such a concept has been used to solve partial differential equations with strong physical background, such as the diffusion equation (Sandev et al., 2018; Lawler, 2010). In our case, we anticipate that the number of water molecules inside a unit volume of soil at any time is also a random process. With this, we can develop a systematic computational framework for solving the Richards equation effectively. Specifically, we use multi-layer neural network to learn a data-driven random walk model, which is then incorporated into a modified FVM scheme to obtain solutions of the Richards equation. Through an illustrative case study, we demonstrate the accuracy and effectiveness of our innovation solution framework and compare it with state-of-the-art numerical methods.

Theoretical Foundation

Preliminaries and Notations

Recall that $\mathbf{K}(\Theta)$ is a highly nonlinear function of moisture content Θ. To model $\mathbf{K}(\Theta)$, a number of empirical correlations have been proposed over the past decades, one of which is proposed by Gardner (1958) as:

$$\Theta(\psi) = \Theta_r + (\Theta_{\text{sat}} - \Theta_r)e^{\alpha\psi}, \tag{3}$$

$$\mathbf{K}(\Theta(\psi)) = \mathbf{K}_{\text{sat}} \frac{\Theta(\psi) - \Theta_r}{\Theta_{\text{sat}} - \Theta_r}, \tag{4}$$

where Θ_r is the residual water content, Θ_{sat} is the water content in saturated soil, α is a constant, and $\mathbf{K}_{\text{sat}}$ is the water conductivity in saturated soil.

Before moving forward, we would like to remark that Equation (1) can also be written as the following pressure head form as we introduce the concept of hydraulic capacity, $C(\psi) := \frac{\partial\Theta}{\partial\psi}$, which itself has been correlated empirically (van Genuchten, 1980):

$$C(\psi)\partial_t\psi + \nabla\cdot\mathbf{q} = 0, \tag{5}$$

From Equation (5), ψ can be explicitly expressed by simply discretizing Equation (1) in a linear scheme, rather than discretizing Equation (5) directly.

Existence and uniqueness of weak solution of the Richards equation

Although in most cases, the exact analytical solution of the Richards equation does not exist, it has been shown that a weak solution to the Richards equation exists and is unique (Misiats and Lipnikov, 2013). A weak solution is a function whose partial derivatives may not all exist but is deemed to satisfy the partial differential equation to be solved in some precisely defined context (Evans, 2010). The existence and uniqueness of weak solution of the Richards equation offers the theoretical guarantee that one can approximate the solution of the Richards equation by constructing its weak solution and solving it numerically. Specifically, we introduce the following valid weak solution of Equation (1), with homogeneous Dirichlet boundary condition given by $\psi(\cdot, z) = 0$ where $z \in \partial\Omega$ and the initial condition given by $\psi(0,\cdot) = \psi_0(\cdot) \in H_0^1(\Omega)$ over $\Omega\times[0,T]$, by applying the implicit Euler method on time domain:

$$\begin{cases} \Theta(\psi^{m+1,s+1}) - \Theta(\psi^m) - \Delta t\mathbf{K}(\Theta(\psi^{m+1,s}))\nabla(\psi^{m+1,s+1} + z) & = 0 \\ \psi^{s+1}|_{z\in\partial\Omega} & = 0 \end{cases} \tag{6}$$

where Δt stands for the time step size (between time steps m and $m+1$), and terms like $\psi^{m+1,s}$ represents the value of ψ at the s-th iteration step of implicit Euler procedure at time step $m+1$. Note that for the initial condition, $H_0^1(\Omega)$ is the completion of $C_0^\infty(\Omega)$ with respect to the Sobolev norm $||\cdot||_1$, where $C_0^\infty(\Omega)$ is the space of infinitely differentiable functions that are nonzero only on a compact subset of Ω. Also, note that other boundary conditions can be easily derived from the homogeneous Dirichlet boundary condition. To show that Equation (6) is a valid weak solution of Equation (1), we refer the readers to the works of Otto (1996) and Misiats and Lipnikov (2013). Furthermore, for $t \in [0,T]$, we have the following result, which can be viewed as the discrete form of Equation (6):

Definition 2.1. *Given* $\psi^s \in H_0^1(\Omega)$, *if for any* $v \in H_0^1(\Omega)$, $\langle\Theta(\psi^{s+1}) - \Theta(\psi^s), v\rangle - \Delta t\langle\, \boldsymbol{K}(\Theta(\psi^{s+1}))\nabla(\psi^{s+1} + z), \nabla v\rangle = 0$, *then* ψ^{s+1} *is a weak solution of Equation* (6).

In addition to this discrete form, one can also derive a continuous form of the weak solution by directly integrating Equation (6) (Misiats and Lipnikov, 2013). From Definition (2.1), it is clear that $\psi^s \in H_0^1(\Omega)$ for every iteration step s. This guarantees that the weak solution of the Richards equation also falls in $H_0^1(\Omega)$, which is the necessary condition to ensure that the numerical solution is valid. Once the existence and uniqueness of weak solution of the Richards equation are shown, we are safe to develop a numerical scheme. Next, we will introduce our novel data-driven random walk algorithm that integrates finite volume discretization and multi-layer neural network.

Discretization Using Finite Volume Method

FVM is a classic numerical method that incorporates conservation laws to allow volume integrals to be converted into surface integrals by applying the divergence theorem (Vinokur, 1989; Barth and Ohlberger, 2003). To demonstrate, we first integrate both sides of Equations (1) and (2) to obtain the integral form of the Richards equation over a $n+1$-dimensional control volume V. Next, we apply the divergence theorem to convert the volume integral into a n-dimensional surface integral after determining the outward pointing unit normal vector $\mathbf{n}$:

$$\int_V \partial_t \Theta(\psi)\mathbf{d}V = \int_V \nabla \cdot [\mathbf{K}(\Theta)\nabla(\psi+z)]\mathbf{d}V. \tag{7}$$

To adopt the FVM, we discretize the control volume V and its surface S_V into N_ω small cells V_i with $i = 1,\cdots,N_\omega$, and small surfaces ω with volume A_ω with $\omega = 1,\cdots,N_\omega$, respectively. Now, to discretize Equation (7), we denote the discretized version of the operator $\mathbf{K}(\cdot)\nabla(\cdot)$ with respect to the small surface ω as $[\mathbf{K}(\cdot)\nabla(\cdot)]_\omega$. The RHS of Equation (7) can be discretized by summing over $[\mathbf{K}(\cdot)\nabla(\cdot)]_\omega$ for all ω:

$$\partial_t \Theta(\psi)\mathrm{vol}(V_i) = \sum_{\omega=1}^{N_\omega} [\mathbf{K}(\Theta)\nabla(\psi+z)]_\omega \cdot \mathbf{n}_\omega A_\omega. \tag{8}$$

To apply time stepping on the LHS of Equation (8), we discretize the time domain and approximate the time derivative $\partial_t\Theta(\psi_i)$ as $\frac{\Theta_i^{m+1,s+1}-\Theta_i^m}{\Delta t}$, where $\Theta_i^{m+1,s+1}$ represents the discretized Θ in the i-th small cell at time step $m+1$ and iteration step $s+1$, and Θ_i^m is the converged Θ value in the i-th small cell at the current time step m. Combining Equations (7) and (8) leads to:

$$\frac{\Theta_i^{m+1,s+1}-\Theta_i^m}{\Delta t}\mathrm{vol}(V_i) = \sum_{\omega=1}^{N_\omega} [\mathbf{K}(\Theta)\nabla(\psi+z)]_\omega \cdot \mathbf{n}_\omega A_\omega. \tag{9}$$

After time stepping is complete, the conventional FVM practice typically writes and solves the discretized equations in matrix form. Due to the stiffness and sparsity of the resulting matrix, solving such a matrix equation is known to be computationally challenging. Therefore, we propose an alternative route that solves the discretized equations in an iterative manner. Inspired from the work of Mitra and Pop (2019), we introduce an adaptive L-scheme by adding the term $L_i^{m+1,s}(\psi_i^{m+1,s+1}-\psi_i^{m+1,s})$ to the LHS of Equation (9). We point out that this adaptive L-scheme is different from the standard L-scheme (Suciu et al., 2021), in which $L_i^{s,m+1}$ is replaced by a non-adaptive constant L. In standard L-scheme, L is arbitrarily chosen and is static subject to changes in Θ at different time step and small cell. In addition, there is no theoretical proof regarding the convergence of standard L-scheme. In fact, the choice of L is not arbitrary and can greatly impact convergence of the L-scheme. On the other hand, for adaptive L-scheme, we have shown that convergence is ensured by $L_i^{m+1,s} \geq \sup|\dot{\Theta}|$ as long as there exists b in which $||\psi_i^0 - \psi_{i-1}^0||_{L^\infty} \leq b\Delta t$. In practice, we select $L_i^{m+1,s}$ to be $\max\{|\ddot{\Theta}(\psi_i^{m+1,s-1})|, 2M\Delta t\}$, for proper $M \geq b\sup|\ddot{\Theta}|$.

Substituting this adaptive L-scheme into Equation (9) yields an adaptive linearized FVM numerical scheme that we use in our algorithm:

$$\begin{aligned}\psi_i^{m+1,s+1} =& \frac{1}{L_i^{m+1,s}}\sum_{\omega=1}^{N_\omega}\mathbf{K}_\omega^{m+1,s}\cdot\mathbf{n}_\omega\frac{(\psi+z)_j^{m+1,s}-(\psi+z)_i^{m+1,s}}{d(j,i)}A_\omega \\ &- \frac{1}{L_i^{m+1,s}}\frac{\Theta_i^{m+1,s+1}-\Theta_i^m}{\Delta t}\mathrm{vol}(V_i) + \psi_i^{m+1,s}.\end{aligned} \tag{10}$$

Data-Driven Random Walk Algorithm

In this section, we introduce the first-of-its-kind data-driven random walk (DRW) algorithm that will be integrated with the FVM scheme to solve the Richards equation. As we will see later, compared to pure FVM-based approaches, the additional underlying physical knowledge implicitly learned by the DRW algorithm can be very useful in obtaining accurate solutions of the Richards equation. Here, we introduce the global random walk procedure, which allows particles to move to neighboring nodes simultaneously instead of one at a time (Vamos et al., 2001). Let $n_i^{m+1,s}$ be the number of particles in cell i at fixed-point iteration step s and time step $m+1$, and $\delta n_{i,j}^{m+1,s}$ be the number of particles moved from cell i to cell j at iteration s and time step $m+1$. Without loss of generality, let us consider the 1-dimensional case in which the number of water molecules in cell i follows:

$$n_i^{m+1,s} = \delta n_{i,i}^{m+1,s} + \delta n_{i+1,i}^{m+1,s} + \delta n_{i-1,i}^{m+1,s}. \tag{11}$$

Vamos et al. (2001) adopted the concept of random walk of particles to solve the diffusion equation. Concentration is modeled simply by taking the arithmetic mean of the number of particles. Authors showed that the random walk solution of the diffusion equation is the same as the solution obtained using finite difference method. While such analogy is intuitive and straightforward to draw when modeling concentration, it cannot be directly extended to the Richards equation which is a highly nonlinear convection-diffusion equation. In other words, the relationship between pressure head ψ_i and the number of particles n_i still remains unclear. In fact, there exists no theoretical guarantee that such as relationship is continuous, smooth, or explicit. Thus, the relationship between ψ_i and n_i may not be describable by any basic function. Therefore, we decide to model the relationship using a multi-layer neural network (MNN), which are known to be possible given that the neural network contains enough neurons (Hornik, 1991). MNN enables us to approximate ψ_i as a nonlinear function of n_i, $\psi_i = f(n_i)$, at any fixed time step and iteration step, which can be incorporated in Equation (9) to yield the following data-driven random walk (DRW) formulation:

$$\begin{aligned}n_i^{m+1,s+1} =& \frac{1}{L_i^{m+1,s}}\sum_{\omega=1}^{N_\omega}\mathbf{K}_\omega^{m+1,s}\cdot\mathbf{n}_\omega\frac{n_j^{m+1,s}-n_i^{m+1,s}}{d(j,i)}A_\omega \\ &+ f^{-1}(\mathbf{J}) + n_i^{m+1,s},\end{aligned} \tag{12}$$

where $\mathbf{J} = \sum_{\omega=1}^{N_\omega} \mathbf{K}_\omega^{m+1,s} \cdot \mathbf{n}_\omega \frac{z_j^{m+1,s} - z_i^{m+1,s}}{d(j,i)} A_\omega - \frac{1}{L_i^{m+1,s}} \frac{\Theta_i^{m+1,s+1} - \Theta_i^m}{\Delta t} \mathrm{vol}(V_i)$. By the reasonable assumptions that $n_i^s \in H_0^1(\Omega)$ and both $\Theta \circ f$ and $\mathbf{K} \circ f$ are $\mathbf{C}^2$ functions with bounded first- and second-order derivatives, one can show that the DRW approach converges to the weak solution of the Richards equation.

DRW Algorithm Architecture

Figure 2 illustrates our DRW architecture. During offline learning, we first obtain reference solutions from the global random walk solvers developed by Suciu et al. (2021) (code available at `https://github.com/PMFlow/FlowBenchmark`). We also add Gaussian noise (Williams, 1995) to these reference solutions to reflect the stochastic nature of the relationship between Ψ_i^s and n_i^s and improve the robustness of DRW algorithm by enhancing its generalization performance. Introducing Gaussian noise also improves the quality of solutions obtained, as the reference solutions themselves exhibit random error and are not strictly accurate. The noise-added reference solutions are used as training and validation sets to train two MNNs, namely MNN1 and MNN2 in Figure 2. In MNN1, we learn f that maps the number of particle in a cell to the pressure head information, whereas in MNN2, we learn the inverse mapping f^{-1} from pressure head information to the number of particles. We point out that even though deep neural network with more layers and neurons could also be used for learning f and f^{-1}, we find MNN with less number of layers (*e.g.,* 3 layers) to be sufficient as long as there is enough neurons in the neural network (Hornik, 1991; Pinkus, 1999).

Once offline learning is complete, we proceed to the actual solution process, where the Richards equation to be solved is first discretized to the adaptive linearized FVM scheme using Equation (10). Then, the discretized form is sent to the DRW algorithm, where it passes through the inverse mapping f^{-1} learned from MNN2 to generate the solution of the Richards equation in terms of the particle distribution in each cell, n_i. Finally, to convert this solution n_i to physically meaningful solutions such as pressure head Ψ, flux q, and moisture content Θ, we apply the trained mapping f. Lastly, we have theoretically proven that the DRW algorithm is convergent, and we use $\varepsilon = \max_i \left\{ \frac{|f(n_i^{s+1}) - f(n_i^s)|}{|f(n_i^{s+1})|} \right\}$ to quantify and monitor the convergence process.

An Illustrative Example

To demonstrate the accuracy and effectiveness of our novel approach, we study the one-dimensional sandy soil example proposed by Schneid et al. (2000) and Suciu et al. (2021). This case study investigates the water flow dynamics within the top 2 meters of the soil (*i.e.,* $\Omega = [0, 2\ \mathrm{m}]$) from $t = 0$ to $t = 10000$ s. We adopt the empirical model of Equations (3) and (4) for $K(\Theta)$ (Gardner, 1958). In this model, we use $K_{\mathrm{sat}} = 2.77 \times 10^{-6}$ m/s, $\Theta_{\mathrm{sat}} = 0.36$, $\Theta_r = 0.06$, and $\alpha = 10$ for sandy soil. For boundary conditions, the water flux is

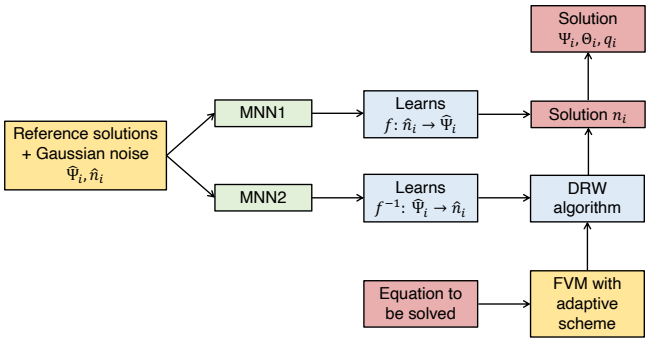

Figure 2: Schmetic of DRW algorithm architecture.

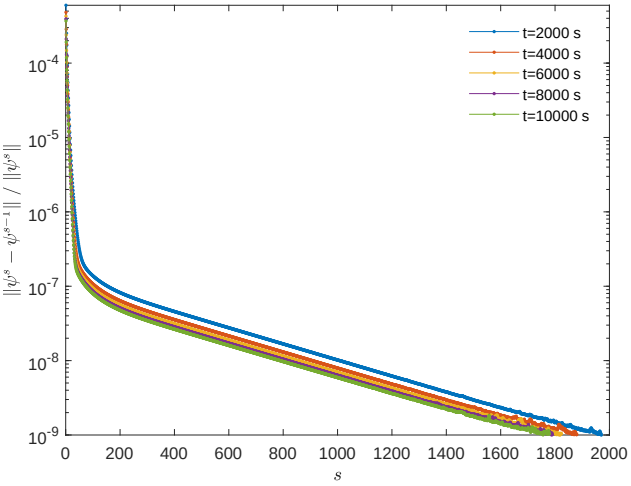

Figure 3: Convergence of DRW algorithm with respect to fixed-point iterations.

2.77×10^{-7} kg/(s·m^2) at $z = 2$ m and $t = 0$ s, and subsequently increases to 2.5×10^{-6} kg/(s·m^2) at $z = 2$ m and $t = 100$ s. And for the initial condition, we assume that the moisture content in Ω is uniform: $\Psi(z,0) = \Psi_0 = 0.5$. The convergence tolerance is set to $\varepsilon = 10^{-9}$. Each of the two neural networks contains a total of 3 layers and 10 neurons. We obtain a total of 1010 noise-added reference solutions from the global random walk solvers (Suciu et al., 2021), with 70% of them used for training, 15% used for validation, and 15% used for testing.

The convergence behavior under various times t (in s) is summarized in Figure 3. Clearly, we observe a stiff convergence rate within the first 100 fixed-point iterations for all times. Convergence rate slows down after that, but still reaches the desired tolerance of 10^{-9} after a total of 2000 iterations. Convergence to fixed-point solutions using implicit Euler for all time steps takes only a few seconds to achieve. Depending on the accuracy requirement of the solution, one may choose a tighter or looser convergence tolerance that balances computational speed and accuracy.

Figures 4, 5, and 6 respectively show the pressure head $\Psi(z,t)$ (in m), soil moisture content $\Theta(z,t)$, and flux $q(z,t)$ (in kg/(s·m^2) solutions of the pressure head form of the Richards equation, Equation (5), at two time stamps: $t = 2000$ s and

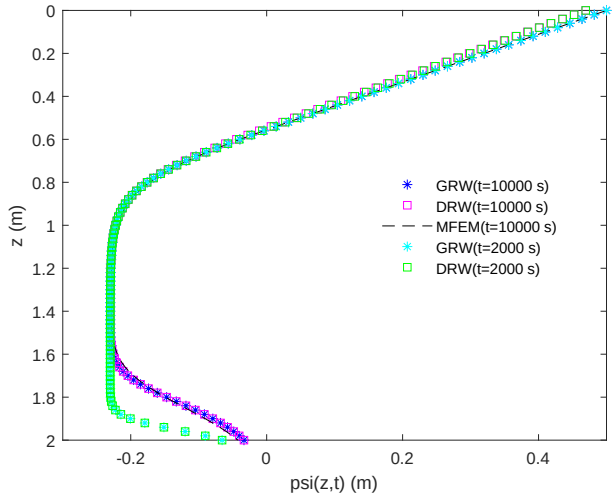

Figure 4: Comparison of pressure head results $\psi(z,t)$ at $t = 2000$ s and $t = 10000$ s.

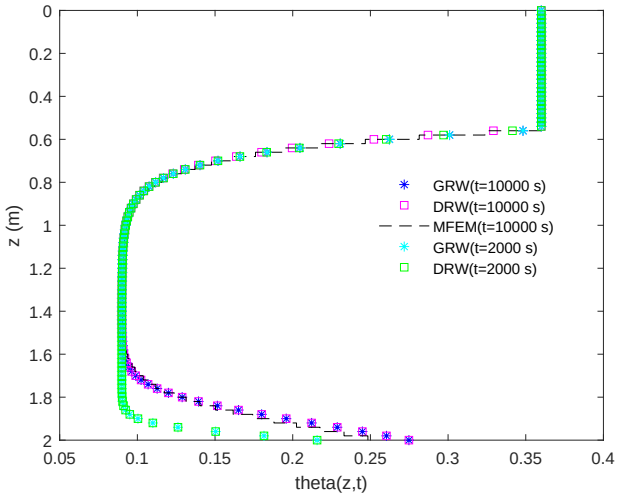

Figure 5: Comparison of soil moisture content results $\Theta(z,t)$ at $t = 2000$ s and $t = 10000$ s.

$t = 10000$ s. In these figures, we compare the solution from our DRW algorithm with two benchmark methods, namely the Global Random Walk (GRW) approach developed by Suciu et al. (2021) and the MFEM framework developed by Schneid et al. (2000). In general, our DRW results show excellent agreement with the GRW results for both time stamps as well as with the MFEM results for $t = 10000$ s, which is the only data set currently available in the literature. Nevertheless, in Figure 6, we observe some inconsistency in the flux results in $z \in [0, 0.8\text{ m}]$. In GRW and MFEM method, the flux remains constant throughout this domain. However, our DRW approach indicates that the flux first stays constant in $z \in [0, 0.6\text{ m}]$, and then decreases during $z \in [0.6, 0.8\text{ m}]$ to a new steady state value that is consistent with what GRW and MFEM give throughout $z \in [0, 0.8\text{ m}]$.

By comparing Figures 5 and 6, one can see that our DRW framework produces the accurate flux results in $z \in [0, 0.8\text{ m}]$. This is because, if the flux stays identical throughout $z \in [0, 0.8\text{ m}]$, then moisture content in Figure 5 should not accumulate or deplete within the same region. Nevertheless, we observe a significant drop in water content from $z = 0.6$ m to $z = 0.8$ m in Figure 5, which exactly matches with the changes in flux from $z = 0.6$ m to $z = 0.8$ m as well. Neither MFEM nor GRW method is capable of learning and utilizing the first-principle knowledge relating flux and soil moisture content. On the other hand, by modeling water flow dynamics as random walk of particles, our DRW approach implicitly learns the underlying physical relationships among different physical properties in the Richards equation as well, which enhances the solution accuracy and interpretability.

Conclusion

Soil moisture is an important hydrological state variable that provides key information which can used in precision agriculture, smart irrigation, drought prevention, weather monitoring. In this work, we develop a novel data-driven random walk (DRW) computational framework to solve the n-dimensional Richards equation, a complex partial differential equation characterizing water flow dynamics in soil. Our DRW approach integrates finite volume discretization, adaptive L-scheme, multi-layer neural networks, and the concept of random walk to enable fast and accurate numerical solution of the Richards equation. We also introduce Gaussian noise to improve the robustness of the DRW framework. To compare our DRW framework with two benchmark numerical methods in the literature, we present an illustrative example of one-dimensional Richards equation. We show that the DRW approach not only generates fast and accurate solutions to the Richards equation, but also implicitly captures the underlying physical relationships among soil moisture content, pressure head, and flux. Future work involves experimental validation of our DRW framework in a 2-acre field located in the Marena, Oklahoma In Situ Sensor Testbed (MOISST) near Stillwater, Oklahoma using in-situ soil moisture sensors.

References

Agyeman, B. T., S. Bo, S. R. Sahoo, X. Yin, J. Liu, and S. L. Shah (2021). Soil moisture map construction by sequential data assimilation using an extended kalman filter. In *2021 American Control Conference (ACC)*, pp. 4351–4356.

Babaeian, E., M. Sadeghi, S. B. Jones, C. Montzka, H. Vereecken, and M. Tuller (2019). Ground, proximal, and satellite remote sensing of soil moisture. *Reviews of Geophysics 57*(2), 530–616.

Barth, T. and M. Ohlberger (2003). Finite volume methods: foundation and analysis.

Cockett, R., L. J. Heagy, and E. Haber (2018). Efficient 3d inversions using the richards equation. *Computers & Geosciences 116*(C), 91–102.

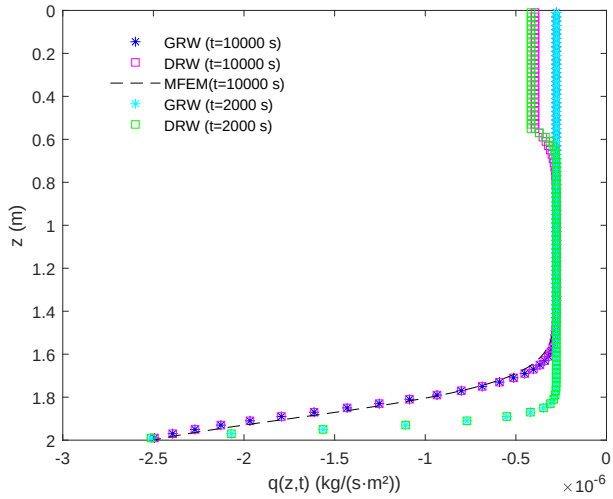

Figure 6: Comparison of flux results $q(z,t)$ at $t = 2000$ s and $t = 10000$ s.

Evans, L. C. (2010). *Partial differential equations*, Volume 19. American Mathematical Soc.

Gardner, W. (1958). Some steady-state solutions of the unsaturated moisture flow equation with application to evaporation from a water table. *Soil science 85*(4), 228–232.

Healy, R. W. (2008). Simulating water, solute, and heat transport in the subsurface with the vs2di software package. *Vadose zone journal 7*(2), 632–639.

Hornik, K. (1991). Approximation capabilities of multilayer feedforward networks. *Neural networks 4*(2), 251–257.

Lawler, G. F. (2010). *Random walk and the heat equation*, Volume 55. American Mathematical Soc.

Misiats, O. and K. Lipnikov (2013). Second-order accurate monotone finite volume scheme for richards' equation. *Journal of Computational Physics 239*, 123–137.

Mitra, K. and I. S. Pop (2019). A modified L-scheme to solve nonlinear diffusion problems. *Computers & Mathematics with Applications 77*(6), 1722–1738.

Mualem, Y. (1976). A new model for predicting the hydraulic conductivity of unsaturated porous media. *Water Resources Research 12*(3), 513–522.

Orouskhani, E., S. R. Sahoo, B. T. Agyeman, S. Bo, and J. Liu (2022). Impact of sensor placement in soil water estimation: A real-case study. *arXiv preprint arXiv:2203.06548*.

Otto, F. (1996). L1-contraction and uniqueness for quasilinear elliptic–parabolic equations. *Journal of Differential Equations 131*(1), 20–38.

Pinkus, A. (1999). Approximation theory of the mlp model in neural networks. *Acta Numerica 8*, 143–195.

Rathfelder, K. and L. M. Abriola (1994). Mass conservative numerical solutions of the head-based richards equation. *Water Resources Research 30*(9), 2579–2586.

Richards, L. A. (1931). Capillary conduction of liquids through porous mediums. *Physics 1*(5), 318–333.

Saavoss, M., J. Majsztrik, B. Belayneh, J. Lea-Cox, and E. Lichtenberg (2016). Yield, quality and profitability of sensor-controlled irrigation: a case study of snapdragon (antirrhinum majus l.) production. *Irrigation science 34*(5), 409–420.

Sandev, T., R. Metzler, and A. Chechkin (2018). From continuous time random walks to the generalized diffusion equation. *Fractional Calculus and Applied Analysis 21*(1), 10–28.

Schneid, E., A. Prechtel, and P. Knabner (2000). A comprehensive tool for the simulation of complex reactive transport and ow in soils.

Simunek, J., M. T. van Genuchten, and M. Sejna (2008). Development and applications of the hydrus and stanmod software packages and related codes. *Vadose zone journal 7*(2), 587–600.

Spelman, D., K.-D. Kinzli, and T. Kunberger (2013). Calibration of the 10HS soil moisture sensor for Southwest Florida agricultural soils. *Journal of Irrigation and Drainage Engineering 139*(12), 965–971.

Suciu, N., D. Illiano, A. Prechtel, and F. A. Radu (2021). Global random walk solvers for fully coupled flow and transport in saturated/unsaturated porous media. *Advances in Water Resources 152*, 103935.

Vamos, C., N. Suciu, H. Vereecken, O. Nitzsche, and H. Hardelauf (2001). Global random walk simulations of diffusion. In *Scientific Computing, Validated Numerics, Interval Methods*, pp. 343–354. Springer.

van Genuchten, M. T. (1980). A closed-form equation for predicting the hydraulic conductivity of unsaturated soils. *Soil Science Society of America Journal 44*(5), 892–898.

Vinokur, M. (1989). An analysis of finite-difference and finite-volume formulations of conservation laws. *Journal of Computational Physics 81*(1), 1–52.

Williams, P. M. (1995). Bayesian regularization and pruning using a Laplace prior. *Neural computation 7*(1), 117–143.